AIAA JOURNAL
Vol. 53, No. 10, October 2015

Improving the Fabrication Process of Micro-Air-Vehicle Flapping Wings

Kelvin Chang,* Anirban Chaudhuri,† Jason Rue,‡ Raphael Haftka,§ and Peter Ifju¶
University of Florida, Gainesville, Florida 32611
and
Christopher Tyler,** Vasishta Ganguly,†† and Tony Schmitz‡‡
University of North Carolina at Charlotte, Charlotte, North Carolina 28223

DOI: 10.2514/1.J053884

The aerodynamic performance of flapping micro air vehicles in hover conditions is dependent on many parameters, including the wing design. With the goal of optimizing the wing for hover performance, the initial focus was to reduce the uncertainty in the thrust measurements. This is because lower uncertainty in this metric enables better resolution in comparing the performance of different designs. Aerodynamic performance variability was deemed to be the fault of an imprecise manufacturing technique. Therefore, adjustments were made to the fabrication process until a permissible level of uncertainty was attained for optimization; the goal was less than 5%. This paper chronicles the progression of the wing fabrication process and details how the uncertainty was evaluated. Four fabrication methods and two different wing designs are included in this study: a carbon fiber hand layup technique, carbon fiber cured in a machined mold, and two variations of a machined plastic skeleton reinforced with a carbon fiber rod. The uncertainty in thrust production, expressed in coefficient of variation, improved from 16.8% for the hand layup method to 2.6% for the computer numerically controlled plastic skeleton adhered to the nylon membrane with transfer tape. Additionally, the coefficient of variation for wing weight also reduced (from 11.4 to 2.0%).

Nomenclature

C_4	=	bias correction factor
CV_{mfg}	=	manufacturing coefficient of variation
CV_{tot}	=	total coefficient of variation
CV_{test}	=	testing coefficient of variation
n	=	samples

I. Introduction

Flapping propulsion for micro air vehicles (MAVs) are an alternative to a fixed wing or rotor-driven configuration. In an environment where there is continued demand for smaller unmanned air vehicles (UAVs), small flapping devices can fly like hummingbirds [1] or even small insects [2,3]. MAVs broadly pertain to flying UAVs that possess no straight dimension longer than 6 in. They have gained popularity for their wide range of applications, including investigation of hazardous environments and spy operations, where size and noise signature are paramount, although designing a UAV in the size range of a hummingbird comes with many challenges. Realization of a mass-produced flapping UAV would likely entail a combination of engineering and affordable materials, where the drive mechanism is simple, light, and durable [4], and the wings are optimized for aerodynamic performance. How do we get there? For the wings, it has been observed that passive deformation from compliance is essential to many of the mechanisms that produce the necessary aerodynamic forces for flight [5]. Also, chordwise flexibility assists in thrust production and efficiency [6]. Thus, the best level of reinforcement for thrust is a compromise between the extremes. Ultimately, a high-fidelity model that incorporates this deformation would be required to optimize the wing skeleton reinforcement design.

A review of different computational models illustrates the breadth of complexity involved in modeling a hovering wing [7], where the advance ratio is zero. Progress has been made in developing validated models [8–11]. However, the complexity of the aeroelastic interaction and highly nonlinear aerodynamics entails exorbitant computational costs or the use of low-fidelity models [12]. This hinders their capability to efficiently predict the aerodynamic performance of a large number of wings, which is important for optimization. The plunge and pitching motions have been optimized for thrust in a slow forward flight flapping airfoil, using a gradient-based optimizer and a two-dimensional model [13]. However, optimization of a wing in hover mode continues to be a challenge. An alternative to using a computation model is to drive the optimization with experiments, using physically measured thrust forces in the place of a high-fidelity model, even possibly looking at tradeoffs between thrust and power measurements [14]. An experimental optimization of the reinforcement structure for hovering flight has been accomplished for thrust alone [15] and with thrust and power as objectives [16]. Techniques such as using different surrogates to have multiple candidate designs every optimization cycle [17] and using an adaptive sampling technique (efficient global optimization) [18] were helpful for minimizing the cost of the optimization, but the main costs pertain to the time spent fabricating and testing wings in a controlled manner. The first major obstacles to accomplishing the optimization was both identifying the uncertainty in the thrust measurement [15] and reducing it to a manageable level by improving the manufacturing techniques used to make the wings. A complete analysis of the uncertainty for different manufacturing methods is provided in this paper. The progression from an inconsistent hand-layup approach to a more precise machine controlled approach is chronicled. It is shown how these improvements reduce

Received 30 August 2014; revision received 16 March 2015; accepted for publication 3 May 2015; published online 23 July 2015.

*Graduate Research Assistant, Department of Mechanical and Aerospace Engineering; kc3635@gmail.com. Student Member AIAA.
†Graduate Research Assistant, Department of Mechanical and Aerospace Engineering; anirban.chaudhuri01@gmail.com. Student Member AIAA.
‡Graduate Research Assistant, Department of Mechanical and Aerospace Engineering; gatorrue@gmail.com.
§Distinguished Professor, Department of Mechanical and Aerospace Engineering; haftka@ufl.edu. Fellow AIAA.
¶Knox T. Millsaps Professor, Department of Mechanical and Aerospace Engineering; ifju@ufl.edu.
**Graduate Research Assistant, Department of Mechanical Engineering and Engineering Science; ctyler6@uncc.edu.
††Graduate Research Assistant, Department of Mechanical Engineering and Engineering Science; v.gang84@gmail.com.
‡‡Professor, Department of Mechanical Engineering and Engineering Science; tony.schmitz@uncc.edu.

the scatter in weight measurements between nominally identical wings and their measured aerodynamic force production.

Earlier work on flapping MAV wings used a flexible wing design [19]. The hand-layup technique used in this study was subsequently extended to a flapping platform [20], tested experimentally, and compared with a computational model [21]. This manufacturing process was also adopted in an experimental investigation of the deformation during flapping [22], recovering the importance of flexibility in the production of aerodynamic thrust force. Many studies use a similar fabrication process, using carbon fiber skeletons with a thin membrane constructed with a combination of hand-assembled and commercially available parts [23–30]. In some cases, extra components like macrofiber composites [31], small check valves [32], and even strain-rate sensors (polyvinylidene fluoride) [33,34] are added. Unfortunately, identification of the uncertainty in the aerodynamic performance from wings made in this manner is commonly overlooked. For example, the performance of a wing could change based on a subtle change in the angle of a spar [35], possibly the result of human error. This paper addresses the uncertainty in the aerodynamic force that is present due to manufacturing variability for wings fabricated in a similar manner to the studies mentioned earlier. A universal approach is detailed for segregating the contribution of manufacturing variability from the total uncertainty, opening this analysis technique to novel approaches in wing fabrication not covered in this paper [36,37]. This paper provides improvements on these commonly used manufacturing techniques along with an approach for identifying the contribution of uncertainty from manufacturing. This can be beneficial to those who use experimental techniques in flapping.

Tests were completed to identify the performance consistency for a series of manufacturing methods; each improving upon the previous. Wing replicates were also tested to compare the various methods for the repeatability of thrust force production. Experiments included 1) 10 tests of the same wing and 2) tests of multiple (10) wings of the same design for each manufacturing method. The former was used to identify the testing repeatability in the absence of manufacturing uncertainty contributions, whereas the latter was used to explore the capability of the selected manufacturing method to produce the same wing in a repeatable manner. Thus, perfect manufacturing repeatability would present as identical scatter in the measurements made in test sets 1 and 2. Weight measurements were taken for each wing, serving as a direct metric of manufacturing repeatability. It is shown to improve with the progression of the manner in which the wings are manufactured.

II. Experimental Procedure and Setup

Four fabrication techniques were analyzed for two reinforcement designs (Figs. 1 and 2); this includes two different frame materials. Because the uncertainty could be driven by the type of wing design, two different wing designs were investigated. The horizontal spar that extends along the top of the wing is called the leading edge (LE), whereas the vertical spar protruding from the triangular corner is called the root batten; these are present in both wing designs. Batten supports emanate radially or vertically downward, comprising the two designs used.

Thrust measurements are the intended metric for aerodynamic performance for the wings and can be thought of as the value of the objective function for optimization. To identify this, the wings were flapped at 20, 25, and 30 Hz with stroke angle amplitude of 96 deg, and the mean aerodynamic force was recorded. The flapping mechanism in Fig. 3 secures the wings at the triangular plate in the base corner of the wing. Every measurement is performed with both wings secured with a screw attachment. The stroke plane and the wing plane are perpendicular when the wings are at rest. There is no hinge in the mechanism to allow for wing rotation at the mount (supination/pronation), and so the wing frame twists during the stroke, relying on the torsional stiffness of the wing for rotation. A dc rotary motor/encoder (Maxon EC16) drives the mechanism, whereas an EPOS 24/1 controller was used to define the flapping frequency via the built-in motor encoder. The mechanism was mounted on a six-

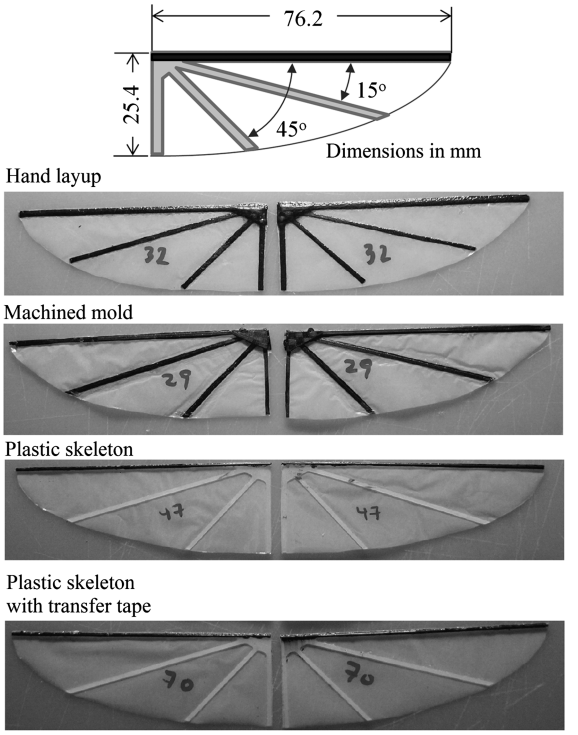

Fig. 1 Four processes are displayed for radial batten wing design along with dimensions of the wing.

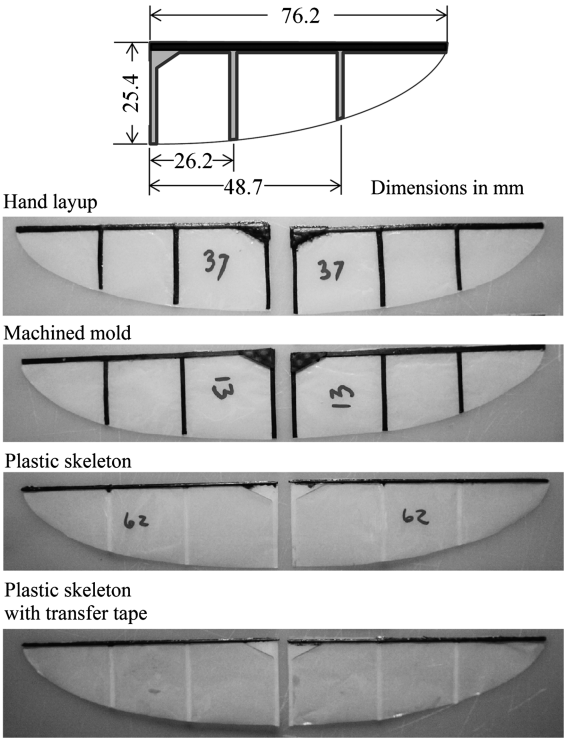

Fig. 2 Four processes are displayed for parallel batten wing design along with dimensions of the wing.

axis force and torque sensor (ATI Industrial Automation Nano17), which was sampled using a 16 bit data acquisition device (National Instruments USB-6251). The Nano17 load sensor is calibrated to resolve down to 0.3 gram force (gf). Both the controller and sensor were managed using LabVIEW virtual instruments. The sampling rate was 30 kHz and a second-order Butterworth low-pass filter was applied with a cutoff frequency of 3 Hz to reduce noise and isolate the steady-state thrust output. A full measurement for one trial of a

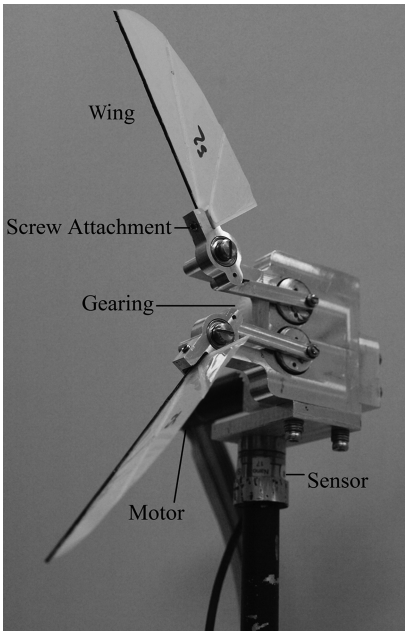

Fig. 3 Flapping mechanism loaded on a six-axis load sensor.

parallel batten wing design is shown in Fig. 4, comparing the raw measurement to the filtered data. As seen in Fig. 4a, the noise overwhelms any prospect of obtaining a time-resolved force contribution from the wings. This is the reason why the average thrust was chosen as the metric of interest.

The data was filtered in real time, allowing the user to quickly identify a wing that had incurred damage. Any wing that was found to have damage was removed from the study. Each trial consisted of a 6 s tare reading to zero the force measurements, followed by a 7 s interval at 20 Hz, and two consecutive 6 s flapping intervals at 25 and 30 Hz. These are commanded frequencies, and so there is an initial ramping stage where the flapping mechanism has yet to obtain the desired frequency. To account for this, the first 2 s of the 20 Hz flapping interval is ignored, and the first second of the 25 and 30 Hz intervals are ignored. The mean force in this interval is used in the uncertainty analysis. Therefore, every wing has one value of thrust for each flapping frequency. Also, the lift force averages close to zero for wings in this study. This is due to the symmetric flapping motion.

III. Fabrication Process

Two different wing designs (shown in Fig. 1) were fabricated using four manufacturing methods. Each of these techniques was used to make multiple replicates, which were nominally identical. For the remainder of this manuscript, these manufacturing methods will be abbreviated as follows:

1) A vacuum-bagged hand layup skeleton bonded to plastic membrane skin with cyanoacrylate (CA) adhesive is referred to as the hand layup.

2) A carbon fiber skeleton made from a machined [computer numerically controlled (CNC)] Teflon® mold and adhered to a plastic membrane skin with CA is called the machined mold.

3) A CNC machined acetal resin skeleton with a channel milled along the leading edge to serve as a locating feature for a commercial-off-the-shelf (COTS) carbon fiber (CF) rod is called a plastic skeleton. The two are bonded with rubber-toughened CA to make the skeleton assembly. Then, the assembly is bonded to the membrane with CA.

4) The plastic skeleton with transfer tape is the same skeleton assembly, differing in that the membrane is adhered with transfer tape as opposed to CA.

The preceding list is the order in which they were devised, each addressing the shortcomings of the previous one. Details of this are provided in the individual descriptions. Common in all the processes is the membrane material. A 14-μm-thick nylon film (Honeywell CAPRAN® 1200 Matte) was used for its minimal weight contribution and strength. Both wing designs (radial and parallel battens) were produced using each manufacturing method to compare the thrust and weight repeatability.

A. Hand Layup Method

The initial method for fabricating the wings involved hand layup of carbon fiber strips on a flat plate, using vacuum pressure to ensure proper consolidation. The preimpregnated (prepreg) unidirectional carbon fiber used in this study incorporated an Aldila AR250 resin system. It was hand cut to approximately 1 mm wide strips, which were then laid onto a rigid aluminum plate with printed placement guides. This is shown in Fig. 5. Three layers were used on the leading-edge spar and one layer was used on the battens. Three layers of bidirectional carbon weave were also cut in triangular shapes to function as the rigid plate for attachment to the flapping device. A similar process was used in the structural deformation study by Keennon and Klingbiel [1]. The wings were cured in an oven following the manufacturer's recommended two-stage curing cycle with a temperate ramp to 190°F and then to 275°F with a hold time of 1 h (2.5 h total, including the ramp times). To assist in consolidation, 30 in Hg of vacuum pressure was applied using a vacuum bag approach for the entire cure cycle. After cure, the frames were carefully removed from the plate. The carbon fiber skeletons were cleared of any cured residual epoxy then adhered to the membrane plastic via CA. The adhesive was applied to the skeleton with a small foam brush and then the skeleton was pressed onto the membrane material. The wing outline was then cut using a knife with the aid of a metal template in the shape of the wing periphery.

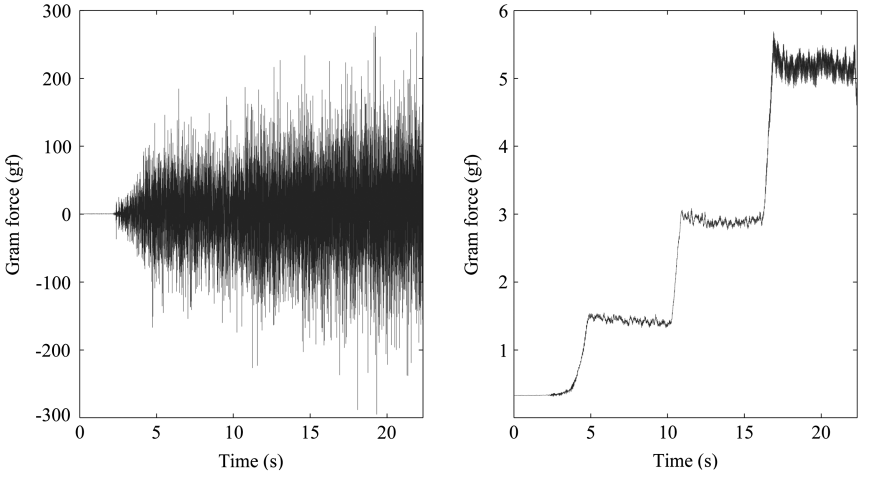

a) **b)**

Fig. 4 Comparison of a) raw thrust measurement and b) filtered thrust measurement for one trial.

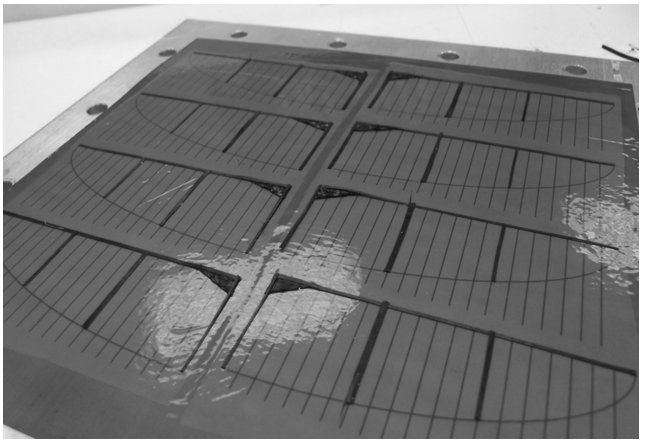

Fig. 5 Parallel batten wings manufactured with hand layup method assembled on a flat plate before curing cycle.

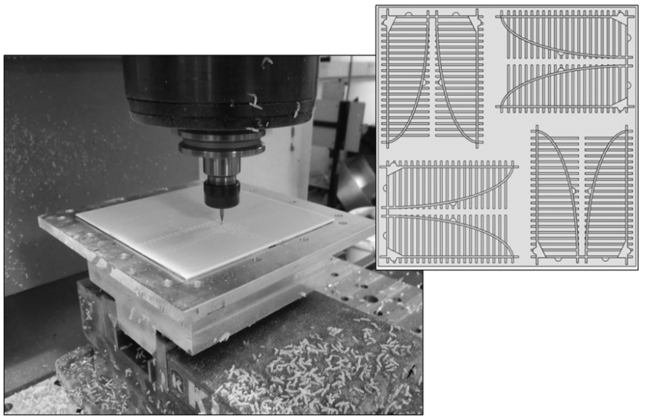

Fig. 6 PTFE sheet is milled with channels for use in machined mold method (a subtractive machining process).

B. Machined Mold Method

The second manufacturing approach was devised with the aim of removing the human error involved in placing the battens. To accomplish this, a CNC-machined polytetraflouroethylene (PTFE, Teflon) mold was used as a base for the unidirectional carbon fiber strips. The topology of each wing frame was CNC machined onto the surface of a 3-mm-thick sheet of PTFE using a 1-mm-diam, four-flute square end mill on a three-axis Haas® TM-1 milling machine (see Fig. 6). The speeds and feeds were chosen to avoid melting and/or plowing of the plastic and to enable proper chip formation. A chip load of 0.07 mm/tooth at the maximum attainable spindle speed of 4000 rpm was selected.

The triangular pockets of the mold held three layers of hand-cut bidirectional carbon fiber; the average thickness of each bidirectional weave layer was approximately 300 μm. Each layer was cut into the shape of right triangles, with sides nominally measured at 6 and 12 mm. The linear channels machined into the mold contained the 1-mm-wide, 130-μm-thick unidirectional carbon fiber strips, the same type used in the hand layup method. To achieve the necessary pressure to bond the layers of the wing assembly, the depth of each mold was undercut in the machining process. The triangular pockets and channels were machined at commanded depths of 340 and 100 μm, respectively. The widths of the channels were machined to be 1 mm, or a 100% radial immersion cut.

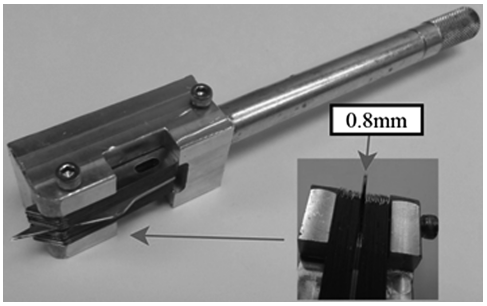

Fig. 7 Custom hand tool configured to cut one fixed width strip of unidirectional prepreg.

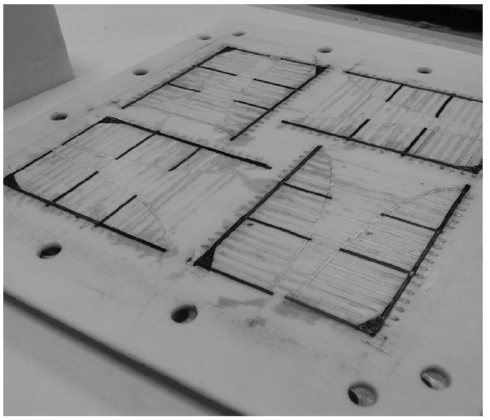

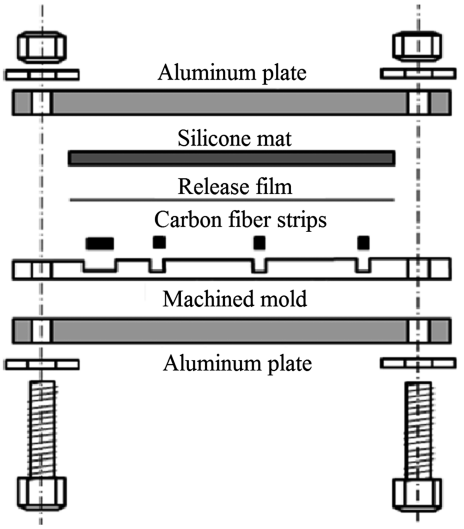

Fig. 8 Exploded view of machined mold.

Controlling the thickness of the battens was another aim of this manufacturing improvement. This was accomplished with a custom hand tool. This bladed device was used to consistently cut the unidirectional strips. It is a hand tool that rigidly holds two cutting blades separated by 0.8 mm. This enabled uniform strips to be cut with each pass (see Fig. 7). This device reduced cutting time and could be configured to cut as many as eight strips side by side. It served to further reduce human error because previous strips were cut using a single blade tool that would be aligned using a straightedge ruler.

The vacuum bag approach was replaced with a sandwich assembly to reduce process time. Once the strips were placed in the channels, a release film (25 μm thick) and a 40A durometer silicone sheet with a thickness of 1.59 mm were placed on top of the strips to provide consolidation pressure. The sandwich assembly was produced by clamping these components between two 6.35-mm-thick aluminum plates. The plates were secured and clamping pressure was applied using 16 screw holes around the periphery to tighten down on the inner layers (see Fig. 8). To reduce warping of the CNC-machined Teflon sheet during the curing process, it was adhered to the aluminum plate using spray adhesive. This eliminated shifting of the PTFE sheet during layup, whereas external pressure supplied from the tightened nuts was responsible for securing the sheet during the curing process. The same oven curing profile as the flat plate method was employed because the same carbon fiber was used. Once cured,

any excess flashing was removed from the skeletons, and they were adhered to the nylon film in the same manner as the hand layup method. In the last step, the periphery was trimmed.

C. Plastic Skeleton Methods

This next manufacturing process involves a larger departure, using a plastic frame as opposed to all carbon fiber. The aim of this approach was to further reduce human-driven errors while attempting to preserve or even improve the wing's thrust production. In this process, a 250-μm-thick sheet of acetal resin (Delrin®) was CNC machined in the shape of the wing skeleton and a COTS 0.5-mm-diam Graphlite® carbon fiber rod was used to reinforce the leading edge. The pultruded carbon fiber rod is specified to have a 67% fiber volume. Acetal resin was chosen due to its good fatigue properties, high stiffness, and machinability. The contour of the wing frame was machined using a 1-mm-diam, four-flute square end mill on a three-axis Haas TM-1 milling machine. Each wing frame was manufactured with a 200-μm-deep, 500-μm-wide channel on the leading edge to locate the carbon fiber rod (see Fig. 9). This was accomplished using a 0.40 mm diameter, four-flute square end mill. The spindle speed (4000 rpm) and feed per tooth (0.07 mm/tooth) were selected to avoid polymer melting during machining. Even though acetal resin has an exceptional natural lubricity, a TiAlN coating was chosen for each cutter to ensure longer cutting life and proper chip evacuation under the full immersion cutting conditions.

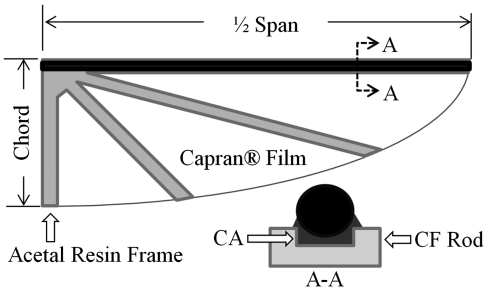

Fig. 9 Plastic skeleton wing construction with cross-sectional geometry of leading edge shown (A-A).

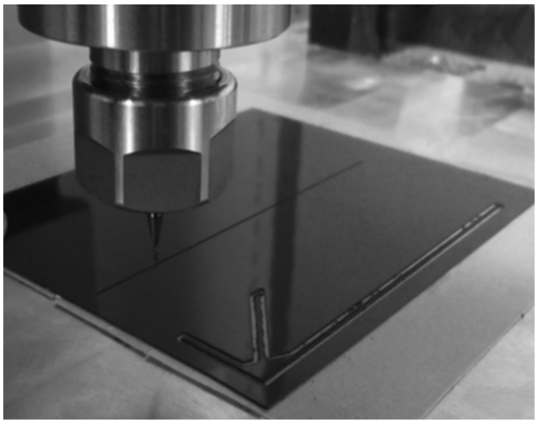

a)

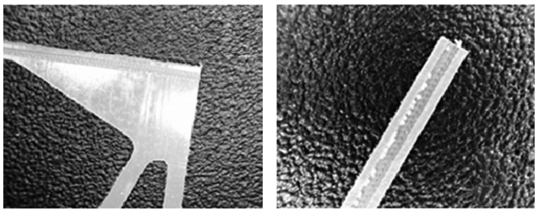

b) **c)**

Fig. 10 CNC process: a) black plastic sheet is milled; b) root area; c) milled channel for carbon fiber rod.

The milling process and resulting plastic wing frames are illustrated in Fig. 10. The carbon fiber rod leading edge was adhered to the plastic frame with CA, the skeleton was adhered to the film with CA, and then the periphery nylon film material was trimmed.

Unfortunately, there were adhesive failures in the bond between the nylon film and plastic skeleton; the final manufacturing improvement addresses this. The last manufacturing process is a variation of the plastic frame approach described earlier. As opposed to using CA, a high-strength acrylic adhesive transfer tape (Scotch® 3M 9471LE 2.3 mil/58 μm thick) was used to adhere the plastic frame to the nylon film. This was incorporated to add compliance and toughness to the bond between the plastic frame and CAPRAN film, making it less prone to failures. As with the previous evolutions, the aim was to sustain thrust force production as well. Extra steps were required for this process, although the overall time was reduced due to the elimination of adhesive curing time. The frame was first placed onto the transfer tape, which consists of a thin film of adhesive (mastic) on a wax paper. The mastic is designed to separate from the wax paper easily. A sheet was used to sandwich the frame (e.g., white copy paper). This step was used to remove the adhesive that was not needed, breaking the edge of the adhesive film (Fig. 11c). At this point, the adhesive was on the frame and there was no adhesive between the battens. The wax paper backing was peeled away to leave the frame with a complete layer of adhesive. Subsequently, the frame was removed and carefully laid onto the nylon film, and then hand pressure was applied to insure uniform adhesion (Fig. 11d). The process of applying the adhesive to the backside of the frame is provided in Figs. 11a–11d as illustrations.

IV. Manufacturing Uncertainty Quantification

The uncertainty quantification for wing thrust measurements outlined by Chaudhuri et al. [15] was used in this work. To quantify the manufacturing uncertainty, the testing uncertainty must be separated from the total uncertainty [Eq. (1)]. To quantify testing uncertainty, the coefficient of variation (CV) of 10 measurements of

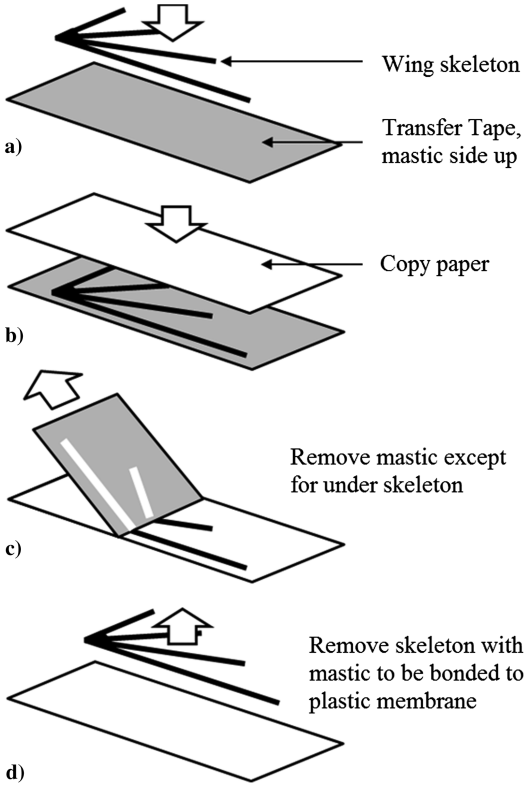

Fig. 11 Adhesive application process: a) skeleton placed on transfer tape; b) copy paper sheet applied, adhering to exposed mastic; c) paper peeled from assembly; and d) skeleton lifted from transfer tape backing, retaining the mastic for adhesion to plastic membrane.

each wing was found. The CV is simply the ratio of the standard deviation to the mean. In this experiment, 10 measurements from each wing were used to determine the mean thrust. This reduced the testing uncertainty in the mean thrust by a factor of $\sqrt{10}$. The root mean square of the reduced coefficients of variation [38,39] was calculated to find the testing uncertainty (CV_{test}).

The total uncertainty (CV_{tot}), which combined the testing and manufacturing uncertainties of the wings, was computed by first taking the mean of 10 measurements, obtaining a mean thrust value for each replicate (sampled manufactured means). Then, the CV of the sampled manufactured means for each design (one for radial and one for parallel) was calculated. These two coefficients of variation were then combined using the root mean square to quantify the CV_{tot}.

The manufacturing uncertainty can be computed by subtracting the testing uncertainty in the mean thrust for each wing from the total uncertainty. However, for small sample sizes, the process of taking the square root of the variance to obtain the standard deviation introduces a bias in the standard deviation estimate [40]. The same applies to the CV because it is the standard deviation over the mean. A simple bias correction can be completed for normal distributions (which was assumed here) using a correction factor [$c_4(n)$, where n is the number of samples] that depends on the sample size [40]. Because of there being 10 replicates available for each design, the corrected coefficient of variation for manufacturing uncertainty (CV_{mfg}) was obtained by dividing by the correction factor for a sample size of 10 [$c4(10) = 0.9727$], which accounts for a 3% increase of the calculated CV. The affect for this correction is minimal for this case, though it can be close to 9% for a sample size of 4:

$$CV_{mfg} = \frac{\sqrt{CV_{tot}^2 - CV_{test}^2}}{c_4(10)} \tag{1}$$

V. Results and Discussion

Finding the proper manufacturing process for the experimental optimization was a matter of identifying a procedure that possesses the smallest uncertainty and is not time intensive, because it is expected that many wings would need to be made for an optimization. Detailed numerical results for each manufacturing process and wing design are provided along with their shortcomings.

A. Thrust Force Uncertainty

For this study, the analysis is limited to 30 Hz flapping frequency, because it represented the upper limit of frequency that the wings could handle without incurring damage on a regular basis. It also introduced the largest testing-based variability and demand on the controller. It also produced a feasible thrust to propel a freestanding hovering device, making it most relevant to a possible application. Table 1 provides a dissected view of CV_{mfg} for each manufacturing process. The values were calculated using Eq. (1) for a 30 Hz commanded flapping frequency. The testing uncertainty is the CV_{test} value divided by $\sqrt{10}$, accounting for the 10 trials for each design.

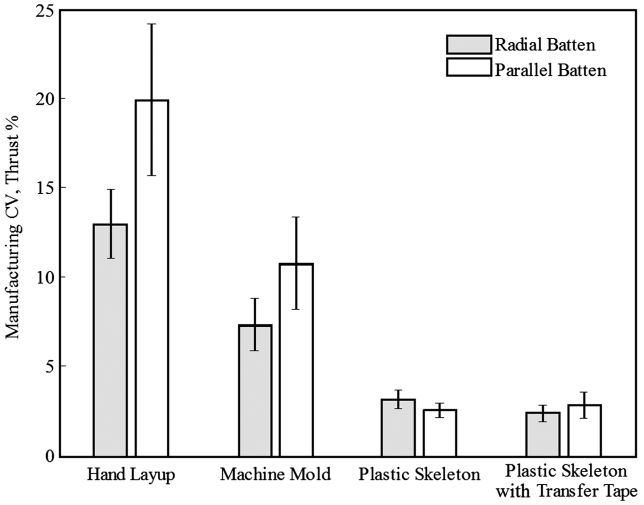

Fig. 12 CV_{mfg} is provided for different manufacturing processes as a percentage.

For clarification, the CV_{test} and CV_{tot} values were formulated from biased standard deviations. As mentioned earlier, they were corrected using $c4(n)$. The manufacturing CV is provided, as a percentage, for each manufacturing process in Fig. 12.

The uncertainty in these results was calculated with a bootstrapping resampling technique, where 5000 datasets were sampled from the original dataset with replacement. This approach provides the sampling distribution for statistics like CV_{tot}. It entails making N datasets from an original set, then calculating the same metric for each all N datasets. This gives a distribution for the metric and was chosen for its simplicity. It assumes that the samples are independent and that they come from the same distribution; there is no normality assumption. The uncertainty value provided in the tables (Tables 1–3) and plots (Figs. 12 and 13) pertain to one standard deviation of the bootstrap distribution of the statistic.

Table 1 shows different mean thrust for each manufacturing method. This is investigated more through observations of the deformation during flapping. The details of this are provided in the Appendix. The differences in mean thrust between the methods can possibly be attributed to the differences in stiffness of the constructions. In subsequent work, the stiffness [41] is characterized for wings made in the plastic construction.

Subtle changes in CV_{tot} were seen for the transfer tape, although adhesive failure of the wings was observed much less frequently with this method. The transfer film was also a faster/easier method for applying the nylon film to the skeleton. The manufacturing improvements assist in realizing wing-specific differences that were previously overwhelmed by larger uncertainties. Therefore, there is more resolution in comparing different designs, which is also important for subsequent optimization [42]. The two design coefficients of variation presented in Table 1 can be combined, using the root mean

Table 1 Thrust CV results for each manufacturing process and design with one standard deviation intervals

	Hand layup	Machined mold	Plastic skeleton	Plastic skeleton with transfer tape
		Radial batten		
Mean thrust, g	5.77	5.49	7.52	7.68
CV_{tot}, %	12.7 ± 1.89	7.19 ± 1.42	3.15 ± 0.50	2.40 ± 0.39
CV_{test}, %	0.67 ± 0.10	0.82 ± 0.07	0.82 ± 0.09	0.74 ± 0.18
CV_{mfg}, %	13.0 ± 1.94	7.3 ± 1.48	3.1 ± 0.54	2.3 ± 0.44
		Parallel batten		
Mean thrust, g	5.73	5.62	7.37	7.70
CV_{tot}, %	19.41 ± 4.11	10.51 ± 2.49	2.52 ± 0.36	2.74 ± 0.72
CV_{test}, %	0.78 ± 0.08	0.79 ± 0.09	0.55 ± 0.05	0.45 ± 0.03
CV_{mfg}, %	19.9 ± 4.2	10.8 ± 2.6	2.5 ± 0.4	2.8 ± 0.8

Note: The calibration error is 0.3 g. This is an additional possible bias.

Table 2 Combined manufacturing uncertainty with one standard deviation intervals

Method	Total uncertainty, CV_{tot}%	Testing uncertainty, CV_{test}%	Manufacturing uncertainty, CV_{mfg}%
Hand layup	16.38 ± 2.41	0.73 ± 0.06	16.8 ± 2.5
Machined mold	9.01 ± 1.54	0.80 ± 0.06	9.2 ± 1.6
Plastic skeleton	2.85 ± 0.31	0.70 ± 0.06	2.8 ± 0.3
Plastic skeleton with transfer tape	2.58 ± 0.41	0.61 ± 0.11	2.6 ± 0.4

Note: The calibration error is 0.3 g. This is an additional possible bias.

Table 3 Weight results with one standard deviation intervals

	Hand layup	Machined mold	Plastic skeleton	Plastic skeleton with transfer tape
		Radial batten		
Average pair discrepancy, g	0.006	0.005	0.006	0.006
Mean weight, g	0.155 ± 0.004	0.158 ± 0.003	0.150 ± 0.002	0.157 ± 0.001
Standard deviation, g	0.012 ± 0.002	0.009 ± 0.002	0.006 ± 0.001	0.004 ± 0.001
CV, %	7.8 ± 1.2	5.7 ± 1.1	4.2 ± 0.8	2.5 ± 0.448
		Parallel batten		
Average pair discrepancy, g	0.011	0.006	0.005	0.002
Mean weight, g	0.153 ± 0.007	0.142 ± 0.001	0.132 ± 0.001	0.135 ± 0.001
Standard deviation, g	0.022 ± 0.004	0.003 ± 0.001	0.003 ± 0.001	0.002 ± 0.000
CV, %	14.2 ± 2.5	1.9 ± 0.5	2.4 ± 0.6	1.4 ± 0.2
		Combined		
CV, %	11.4 ± 1.5	4.3 ± 0.7	3.5 ± 0.5	2.0 ± 0.3

square to compare the different manufacturing techniques. This is presented in Table 2. The testing uncertainty, contributing less to the total uncertainty, was found to vary little between manufacturing processes.

This is expected because no intended modifications to the process of testing the wings were made between any of the tests, although the subtle changes could be attributed to diversity in the mounting or fatigue of the wing between trials, all of which could be specific to the manufacturing process used to make the wing. The results show a sixfold improvement of manufacturing uncertainty when the radial and parallel batten statistics are combined.

B. Weight Uncertainty

The weight of each of the 160 wings (80 wing pairs) varied with both the manufacturing method and design. Each individual wing was measured with a Gemini-20 portable milligram scale and less scatter was observed with each manufacturing progression (Table 3). The average pair discrepancy pertains to the weight difference between the left and right wings. A reduction in weight discrepancy is present for the parallel design, though it does not fluctuate for the radial batten wing design. The weight of the plastic skeleton wings compare with those used on the Saturn prototype, a long-endurance variation of the Nano Hummingbird, which possesses 0.26 g for a pair of wings, making each wing weigh approximately 0.13 g; both wings pertain to 1% of the flier's total weight [1].

The CV for both designs and all four manufacturing processes is presented in Fig. 14. Each bar entails 20 independent wing measurements (10 pairs); the plot covers every combination of fabrication process and wing design.

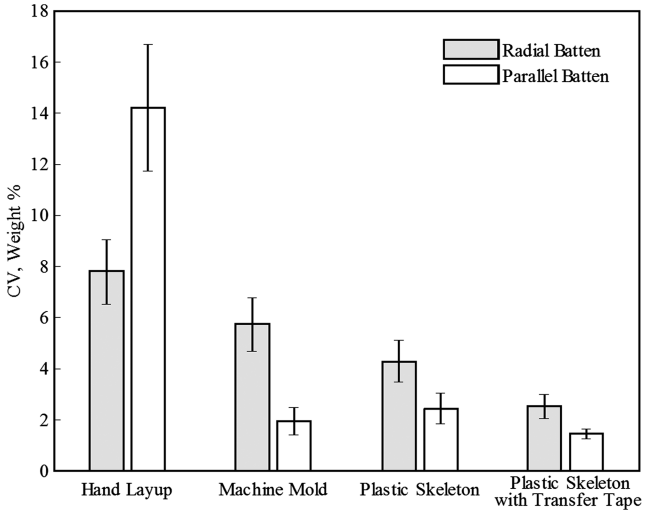

Fig. 13 Weight CV categorized by manufacturing process and design.

C. Cross-Sectional Geometry

From visual inspection, the hand layup approach exhibited the most cross-sectional variation. Distortion of the cross section was due to external pressure applied from the vacuum bag, resulting in a curved geometry; this is visible in Fig. 14. This deformation was consistently present and is likely a key contributor to the variability seen in the thrust performance. Though the widened base of the cross section provides more surface area to promote adhesion, it reduces the second moment of area and thus the bending stiffness in an uncontrolled manner; this makes for varying levels of deformation during flapping, accompanied by differences in the thrust performance in nominally identical wings.

The next progression was the machined mold approach which, from visual inspection, successfully controlled batten thicknesses and improved the precision of the batten placement. The machined mold provided constraining channel walls that deterred batten movement during the curing cycle. The wing frame, fabricated from the machined mold process, possessed a defined leading edge and more consistent geometric shape. These improvements are reflected in both the weight CV and thrust force CV compared with the hand layup process. By using machined channels, consistency in the batten

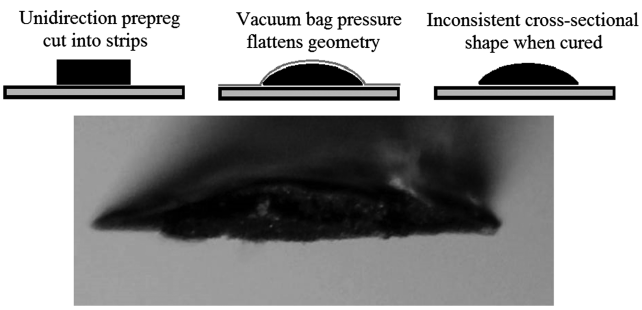

Fig. 14 Uncontrolled geometric changes of LE spar due to vacuum bag curing process. Progression shows view of LE cross section.

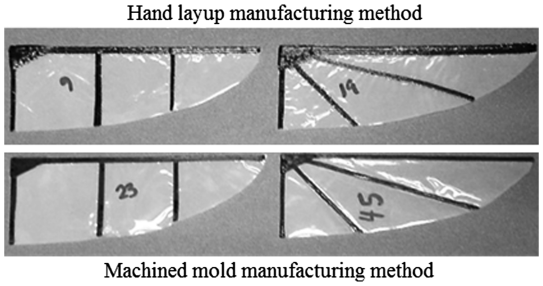

Fig. 15 Comparison of wings made with hand layup and machined mold manufacturing methods.

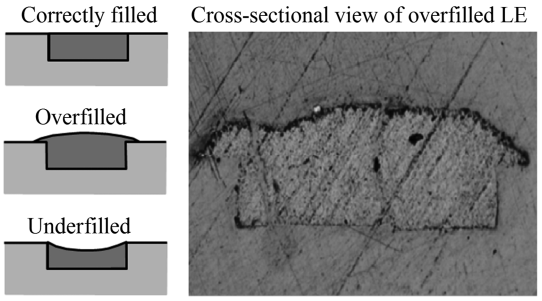

Fig. 16 Typical defects occur when either the mold is under- or overfilled. Microscope still shows a leading edge that was sectioned.

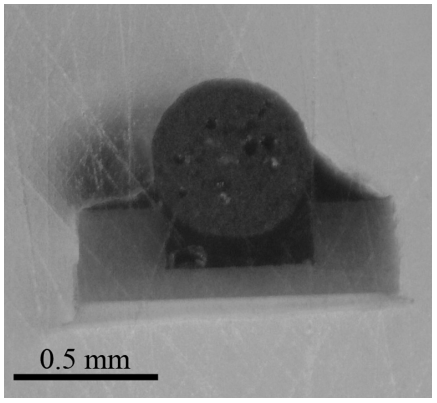

Fig. 17 Magnified view of cross section where leading edge carbon fiber spar is adhered to plastic skeleton.

placement was achieved, and reduced distortion of the cross-sectional geometry was visible; this is shown in Fig. 15. Another contributor to the batten width consistency is the comb cutter hand tool. It prepared strips of unidirectional carbon fiber with uniform thickness, a visual improvement over a single blade hand-cutting tool used with a straightedge.

The shortcomings of the machined mold approach were based on inconsistency at the unconstrained surface, where the wing's frame does not touch the mold's walls (interfaces with release film). Under- and overfilling of the channels of the carbon was observed. A combination of insufficient channel depth, inconsistent pressure, and variations in the amount of carbon in the channel were responsible for the geometries displayed in Fig. 16. The flatness of this face is important for an even bond to the nylon film, and so adhesive failures were seen more frequently as compared with the hand layup wings. This top face would often cure to a curved shape as shown in Fig. 16 (underfilled) causing voids/bubbles in the bond line where cohesive failure would emanate. The sensitivity of the interplay between the applied pressure, channel depth, and amount of carbon fiber placed into the mold was found to produce an inconsistent top surface geometry. Increasing the machining accuracy would possibly improve this, though it would add considerably to machining time and costs.

The plastic skeleton wings, machined with a CNC, provided the least scatter in the thrust and weight. The introduction of a transfer tape adhesive to bond the nylon film to the frame introduced minimal improvements to the scatter, although it was the most durable construction, reducing fabrication time and complexity. The failures seen in wings using CA were likely due to the low surface energy of the Delrin, which hinders adhesion, and the brittle nature of CA, resulting in cohesive failure. The adhesion of the leading-edge carbon rod is shown in Fig. 17, where the CA adhesive fills the rectangular channel and interfaces with the sides as well. This is the result of wicking, where the excess CA is sometimes visible on the top surface of the plastic skeleton; it provides more surface area for the adhesive to bond to.

VI. Conclusions

With reduced uncertainty in average thrust, smaller differences in thrust due to design variations can be resolved. This reduction is especially important for application to experimental optimization, where surrogates of the thrust performance (with respect to design variables) take into consideration the level of uncertainty in the measurements when fitting the data. The manufacturing process used to fabricate the flapping wings will continuously evolve, though it has developed to a level, based on uncertainty analysis, that is worthy of an experimental optimization. The weight, measured for all of the wings tested, revealed lower uncertainty with the progressive improvements of the manufacturing method. Through extensive testing of 80 wing pairs, it has been shown that the CV was reduced by more than 6 times with manufacturing process improvements that incorporate more precise techniques and materials. This includes testing of two different wing designs, showing that the uncertainty measures vary less with improved manufacturing methods. A CNC-machined acetal resin frame attached to a nylon film with transfer film adhesive was found to have the least manufacturing uncertainty. This approach was the product of successive fabrication process improvements, some of which were compared here. The repeatability obtained through these methods was the result of carefully followed procedures. Therefore, small details of the process were provided. There is hope that the improvements and this analysis can be used as a framework for others to interrogate the suitability of specific manufacturing methods to produce repeatable performance in flapping wing tests of all types, including those not covered in this work. As it stands, this is the most comprehensive prospective study of manufacturing uncertainty in flapping wings and how various techniques affect aerodynamic force measurements. In subsequent work, the authors implemented a power consumption metric along with an uncertainty analysis so that efficiency can be used as an objective in an optimization. Also, the stiffness was characterized for different designs in the optimizations. In future work, deformation throughout the flap cycle will be measured to recover the characteristics of high-thrust performance wings.

Appendix: Wing Deformation Study

A separate study was conducted to observe the pattern of deformation slightly after stroke reversal, where deformation was maximum. This was done to help understand the increase in mean thrust with the introduction of a plastic frame construction. The full-field deformation results seen in Fig. A1 were captured using digital image correlation at approximately 5 deg from the stroke reversal, where the out-of-plane deformation was found to be greatest. A pair of Point Grey Research Flea2® cameras were used along with Correlated Solution's VIC-3D™ software. The wing was painted black and speckled with white enamel paint in a thin coat. Measurements were taken on wings flapped at 25 Hz, because 30 Hz flapping frequency made for excessive deformation, where the membrane would orient out of the cameras' view, making for poor correlation.

Figure A1 shows the deflection of parallel batten wings in three different constructions. Here, the plastic wing is one where the frame was attached to the membrane with transfer tape. The CA-adhered

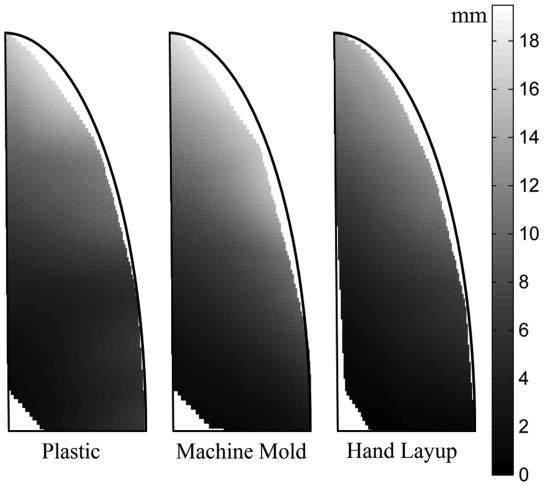

Fig. A1 Displacement plots for three wing constructions.

variation was neglected because its construction is similar. The plot shows the out-of-plane deflection of the wings, and the white segments on the trailing edge pertain to unmeasured regions (due to glare and folding of the membrane during flapping). The hand layup wing had the least leading-edge tip deflection and the machine mold wing had the most. The plastic distinguishes itself with deflection at the root of the wing, indicating more twist throughout the body. This suggests that twisting throughout the length of the wing body has positive effects on the average thrust.

Acknowledgments

This work was supported by the U.S. Air Force Office of Scientific Research grant FA9550-11-1-0066 from David Stargel, Grant Monitor. Also, thanks to Jordan Van Hall for his manufacturing and testing contributions.

References

[1] Keennon, M., and Klingebiel, K., "Development of the Nano Hummingbird: A Tailless Flapping Wing Micro Air Vehicle," *AIAA Aerospace Sciences Meeting*, AIAA, Reston, VA, 2012, pp. 1–24.

[2] Wood, R. J., "First Takeoff of a Biologically Inspired At-Scale Robotic Insect," *IEEE Transactions on Robotics*, Vol. 24, No. 2, 2008, pp. 341–347.
doi:10.1109/TRO.2008.916997

[3] Ma, K. Y., and Felton, R. J., "Wood, Design, Fabrication, and Modeling of the Split Actuator Microrobotic Bee," *2012 IEEE/RSJ International Conference on Intelligent Robots and Systems*, IEEE Publ., Piscataway, NJ, 2012, pp. 1133–1140.
doi:10.1109/IROS.2012.6386192

[4] Bejgerowski, W., Ananthanarayanan, A., Mueller, D., and Gupta, S. K., "Integrated Product and Process Design for a Flapping Wing Drive Mechanism," *Journal of Mechanical Design*, Vol. 131, No. 6, 2009, Paper 061006.
doi:10.1115/1.3116258

[5] Mountcastle, A. M., and Daniel, T. L., "Aerodynamic and Functional Consequences of Wing Compliance," *Experiments in Fluids*, Vol. 46, No. 5, 2009, pp. 873–882.
doi:10.1007/s00348-008-0607-0

[6] Heathcote, S., and Gursul, I., "Flexible Flapping Airfoil Propulsion at Low Reynolds Numbers," *AIAA Journal*, Vol. 45, No. 5, 2007, pp. 1066–1079.
doi:10.2514/1.25431

[7] Shyy, W., Aono, H., Chimakurthi, S. K., Trizila, P., Kang, C.-K., Cesnik, C. E. S., and Liu, H., "Recent Progress in Flapping Wing Aerodynamics and Aeroelasticity," *Progress in Aerospace Sciences*, Vol. 46, No. 7, 2010, pp. 284–327.
doi:10.1016/j.paerosci.2010.01.001

[8] Gordnier, R. E., Kumar Chimakurthi, S., Cesnik, C. E. S., and Attar, P. J., "High-Fidelity Aeroelastic Computations of a Flapping Wing with Spanwise Flexibility," *Journal of Fluids and Structures*, Vol. 40, July 2013, pp. 86–104.
doi:10.1016/j.jfluidstructs.2013.03.009

[9] Ansari, S. A., Żbikowski, R., and Knowles, K., "Non-Linear Unsteady Aerodynamic Model for Insect-Like Flapping Wings in the Hover. Part 1: Methodology and Analysis," *Journal of Aerospace Engineering*, Vol. 220, No. 2, 2006, pp. 61–83.
doi:10.1243/09544100JAERO49

[10] Gogulapati, A., Friedmann, P. P., Kheng, E., and Shyy, W., "Approximate Aeroelastic Modeling of Flapping Wings in Hover," *AIAA Journal*, Vol. 51, No. 3, 2013, pp. 567–583.
doi:10.2514/1.J051801

[11] Pourtakdoust, S. H., and Aliabadi, S. K., "Evaluation of Flapping Wing Propulsion Based on a New Experimentally Validated Aeroelastic Mode," *Scientia Iranica*, Vol. 19, No. 3, 2012, pp. 472–482.
doi:10.1016/j.scient.2012.03.004

[12] Stanford, B., Kurdi, M., Beran, P., and McClung, A., "Shape, Structure, and Kinematic Parameterization of a Power-Optimal Hovering Wing," *Journal of Aircraft*, Vol. 49, No. 6, 2012, pp. 1687–1699.
doi:10.2514/1.C031094

[13] Tuncer, I., and Kaya, M., "Optimization of Flapping Airfoils for Maximum Thrust," *AIAA Journal*, Vol. 43, No. 11, 2005, pp. 2329–2336.
doi:10.2514/1.816

[14] Chaudhuri, A., Haftka, R., Chang, K., Van Hall, J., and Ifju, P., "Thrust-Power Pareto Fronts Based on Experiments of a Small Flapping Wing," *10th AIAA Multidisciplinary Design Optimization Conference*, AIAA, Reston, VA, 2014, pp. 1–9.

[15] Chaudhuri, A., Haftka, R. T., Ifju, P., Chang, K., Tyler, C., and Schmitz, T., "Experimental Flapping Wing Optimization and Uncertainty Quantification Using Limited Samples," *Structural and Multidisciplinary Optimization*, Vol. 51, No. 4, 2015, pp. 957–970.
doi:10.1007/s00158-014-1184-x

[16] Chaudhuri, A., Chang, K., Haftka, R., and Ifju, P., "Multi-Objective Experimental Optimization with Multiple Simultaneous Sampling for Flapping Wings," *56th AIAA/ASCE/AHS/ASC Structures, Structural Dynamics, and Materials Conference*, AIAA, Reston, VA, 2014, pp. 1–17.
doi: 10.2514/6.2015-1586

[17] Viana, F., and Haftka, R., "Efficient Global Optimization with Experimental Data: Revisiting the Paper Helicopter Design," *52nd AIAA/ASME/ASCE/AHS/ASC Structures, Structural Dynamics, and Materials Conference*, AIAA, Reston, VA, 2011, pp. 1–21.

[18] Jones, D., Schonlau, M., and Welch, W., "Efficient Global Optimization of Expensive Black-Box Functions," *Journal of Global Optimization*, Vol. 13, No. 4, 1998, pp. 455–492.
doi:10.1023/A:1008306431147

[19] Ifju, P., Jenkins, D., Ettinger, S., and Lian, Y., "Flexible-Wing-Based Micro Air Vehicles," AIAA Paper 2002-0705, 2002.

[20] Wu, P., Ifju, P., and Stanford, B., "Flapping Wing Structural Deformation and Thrust Correlation Study with Flexible Membrane Wings," *AIAA Journal*, Vol. 48, No. 9, 2010, pp. 2111–2122.
doi:10.2514/1.J050310

[21] Wu, P., Sällström, E., Ukeiley, L., Ifju, P., Chimakurthi, S., Aono, H., Cesnik, C. E. S., and Shyy, W., "Integrated Experimental and Computational Approach to Analyze Flexible Flapping Wings in Hover," *Conference Proceedings of the Society of Experimental Mechanics*, Soc. for Experimental Mechanics, Bethel, CT, 2011, pp. 1441–1451.
doi:10.1007/978-1-4419-9834-7

[22] Wu, P., Stanford, B. K., Sällström, E., Ukeiley, L., and Ifju, P. G., "Structural Dynamics and Aerodynamics Measurements of Biologically Inspired Flexible Flapping Wings," *Bioinspiration and Biomimetics*, Vol. 6, No. 1, 2011, Paper 016009.
doi:10.1088/1748-3182/6/1/016009

[23] Nakata, T., Liu, H., Tanaka, Y., Nishihashi, N., Wang, X., and Sato, A., "Aerodynamics of a Bio-Inspired Flexible Flapping-Wing Micro Air Vehicle," *Bioinspiration & Biomimetics*, Vol. 6, No. 1, 2011, Paper 045002.
doi:10.1088/1748-3182/6/4/045002

[24] Mueller, D., Bruck, H. A., and Gupta, S. K., "Measurement of Thrust and Lift Forces Associated with Drag of Compliant Flapping Wing for Micro Air Vehicles Using a New Test Stand Design," *Experimental Mechanics*, Vol. 50, No. 6, 2009, pp. 725–735.
doi:10.1007/s11340-009-9270-5

[25] Fenelon, M., and Furukawa, T., "Design of an Active Flapping Wing Mechanism and a Micro Aerial Vehicle Using a Rotary Actuator," *Mechanism and Machine Theory*, Vol. 45, No. 2, 2010, pp. 137–146.
doi:10.1016/j.mechmachtheory.2009.01.007

[26] Shkarayev, S., Maniar, G., and Shekhovtsov, A. V., "Experimental and Computational Modeling of the Kinematics and Aerodynamics of

Flapping Wing," *Journal of Aircraft*, Vol. 50, No. 6, 2013, pp. 1734–1747.
doi:10.2514/1.C032053

[27] Mazaheri, K., and Ebrahimi, A., "Experimental Investigation of the Effect of Chordwise Flexibility on the Aerodynamics of Flapping Wings in Hovering Flight," *Journal of Fluids and Structures*, Vol. 26, No. 4, 2010, pp. 544–558.
doi:10.1016/j.jfluidstructs.2010.03.004

[28] Hu, H., Kumar, A. G., Abate, G., and Albertani, R., "Experimental Investigation on the Aerodynamic Performances of Flexible Membrane Wings in Flapping Flight," *Aerospace Science and Technology*, Vol. 14, No. 8, 2010, pp. 575–586.
doi:10.1016/j.ast.2010.05.003

[29] Yoon, S., Kang, L., and Jo, S., "Development of Air Vehicle with Active Flapping and Twisting of Wing," *Journal of Bionic Engineering*, Vol. 8, No. 1, 2011, pp. 1–9.
doi:10.1016/S1672-6529(11)60007-3

[30] Nguyen, Q. V., Truong, Q. T., Park, H. C., Goo, N. S., and Byun, D., "Measurement of Force Produced by an Insect-Mimicking Flapping-Wing System," *Journal of Bionic Engineering*, Vol. 7, Sept. 2010, pp. S94–S102.
doi:10.1016/S1672-6529(09)60222-5

[31] Kim, D.-K., Kim, H.-I., Han, J.-H., and Kwon, K.-J., "Experimental Investigation on the Aerodynamic Characteristics of a Bio-Mimetic Flapping Wing with Macro-Fiber Composites," *Journal of Intelligent Material Systems and Structures*, Vol. 19, No. 3, 2007, pp. 423–431.
doi:10.1177/1045389X07083618

[32] Ho, S., Nassef, H., Pornsinsirirak, N., Tai, Y.-C., and Ho, C.-M., "Unsteady Aerodynamics and Flow Control for Flapping Wing Flyers," *Progress in Aerospace Sciences*, Vol. 39, No. 8, 2003, pp. 635–681.
doi:10.1016/j.paerosci.2003.04.001

[33] Raney, D. L., and Slominski, E. C., "Mechanization and Control Concepts for Biologically Inspired Micro Air Vehicles," *Journal of Aircraft*, Vol. 41, No. 6, 2004, pp. 1257–1265.
doi:10.2514/1.5514

[34] Yang, L.-J., Hsu, C.-K., Ho, J.-Y., and Feng, C.-K., "Flapping Wings with PVDF Sensors to Modify the Aerodynamic Forces of a Micro Aerial Vehicle," *Sensors and Actuators A: Physical*, Vol. 139, Nos. 1–2, 2007, pp. 95–103.
doi:10.1016/j.sna.2007.03.026

[35] Gerdes, J. W., Cellon, K. C., Bruck, H. A., and Gupta, S. K., "Characterization of the Mechanics of Compliant Wing Designs for Flapping-Wing Miniature Air Vehicles," *Experimental Mechanics*, Vol. 53, No. 9, 2013, pp. 1561–1571.
doi:10.1007/s11340-013-9779-5

[36] Pornsin-Sirirak, T. N., Tai, Y. C., Nassef, H., and Ho, C. M., "Titanium-Alloy MEMS Wing Technology for a Micro Aerial Vehicle Application," *Sensors and Actuators A: Physical*, Vol. 89, Nos. 1–2, 2001, pp. 95–103.
doi:10.1016/S0924-4247(00)00527-6

[37] Laliberté, J. F., Kraemer, K. L., Dawson, J. W., and Miyata, D., "Design and Manufacturing of Biologically Inspired Micro Aerial Vehicle Wings Using Rapid Prototyping," *International Journal of Micro Air Vehicles*, Vol. 5, No. 1, 2013, pp. 15–38.
doi:10.1260/1756-8293.5.1.15

[38] Gluer, C., Blake, G., Lu, Y., Blunt, B. A., Jergas, M. I., and H. K., Genant, "Accurate Assessment of Precision Errors: How to Measure the Reproducibility of Bone Densitometry Techniques," *Osteoporosis International*, Vol. 5, No. 4, 1995, pp. 262–270.
doi:10.1007/BF01774016

[39] Dransfield, R. D., and Brightwell, R., "How to Get on Top of Statistics: Design and Analysis for Biologists, with R. InfluentialPoints," 2012, http://www.influentialpoints.com/.

[40] Trietsch, D., *Statistical Quality Control: A Loss Minimization Approach*, World Scientific, River Edge, NJ, 1999.

[41] Chang, K., Chaudhuri, A., Tang, J., Van Hall, J., Ifju, P., Haftka, R., Tyler, C., and Schmitz, T., "Stiffness Investigation of Synthetic Flapping Wings for Hovering Flight," *Advancement of Optical Methods in Experimental Mechanics*, Springer International, New York, 2015, pp. 249–256.
doi:10.1007/978-3-319-06986-9_28

[42] Chang, K., Rue, J., Ifju, P., Haftka, R., Schmitz, T., Tyler, C., Chaudhuri, A., and Ganguly, V., *Analysis of Thrust Production in Small Synthetic Flapping Wings*, Springer International, New York, 2014, pp. 1–8.
doi:10.1007/978-3-319-00876-9

N. Wereley
Associate Editor